



Study of the active site for acetylene hydrochlorination in AuCl₃/C catalysts



Songlin Chao^a, Qingxin Guan^a, Wei Li^{a,b,*}

^a Key Laboratory of Advanced Energy Materials Chemistry (Ministry of Education), College of Chemistry, Nankai University, Tianjin 300071, China

^b Collaborative Innovation Center of Chemical Science and Engineering (Tianjin), Nankai University, Tianjin 300071, China

ARTICLE INFO

Article history:

Received 4 April 2015

Revised 26 June 2015

Accepted 2 July 2015

Keywords:

Acetylene hydrochlorination

Active site

Temperature-programmed desorption

Au

Activated carbon

ABSTRACT

AuCl₃/C catalysts were prepared using activated carbon pretreated at different temperatures. The set of catalysts was evaluated for acetylene hydrochlorination, and the most stable catalyst exhibited the weakest acetylene adsorption capacity, as characterized by the method of temperature-programmed desorption (TPD). The catalysts were also investigated using X-ray diffraction, X-ray photoelectron spectroscopy, Fourier transform infrared spectroscopy, and other methods. It is shown that the activated carbon works as a constituent part of the active site that is responsible for the activation of acetylene. The result provides evidence for the assumption that the Au³⁺ at the AuCl₃/C interface of the catalyst is the active site of the classical AuCl₃/C catalyst.

© 2015 Elsevier Inc. All rights reserved.

1. Introduction

Vinyl chloride monomer (VCM) is an important chemical raw material that is used to manufacture polyvinylchloride. Because of China's abundant coal reserves, the manufacture of VCM is primarily performed via acetylene hydrochlorination, by means of HgCl₂ supported on activated carbon as the catalyst [1,2]. Because HgCl₂ is toxic and apt to sublime, HgCl₂ supported catalysts have a relatively short lifetime and are environmentally hazardous [3].

The pioneering work and systematic studies carried out by Hutchings and co-workers showed that supported AuCl₃ catalysts would be viable catalysts for acetylene hydrochlorination [3–6]. Hutchings et al. demonstrated that Au³⁺ played a crucial role in the reaction, and the reduction of Au³⁺ to Au⁰ during the reaction caused deactivation of the catalyst [4,7–10]. In addition, recent research has shown that an excess of Au³⁺ does not contribute to catalytic activity, and the location of Au³⁺ at the AuCl₃/C interface of the catalyst is likely to be related to the efficiency of the catalyst [7,11].

Moreover, several metal-free catalysts have been reported recently [12–14]. Bao et al. reported a nanocomposite obtained

by growing an N-doped carbon layer out of preshaped silicon carbide granules as the catalyst for acetylene hydrochlorination, and demonstrated that the carbon atoms bonded to pyrrolic nitrogen atoms are the active sites [13]. Wei et al. reported that N-doped carbon nanotubes are activated for the reaction, based on the consideration that the electron affinity of carbon can be tuned as the active metal cation for acetylene hydrochlorination by doping [15].

In spite of the outstanding work that has been reported, the active site of the classic supported gold catalyst is still not clear. The previous work mentioned above inspired us consider that the activated carbon may play a central role in the overall reaction mechanism of AuCl₃/C catalysts. Activated carbon has abundant surface functional groups that could affect the reaction mechanism and are easily modified by suitable thermal or chemical post-treatments [16,17]. This prompted us to investigate the effect of activated carbon's surface functional groups by modifying activated carbon using a thermal treatment that will not add new elements.

Therefore, we modified the surface functional groups on activated carbon to achieve a change in catalytic performance. The activity was examined using X-ray photoelectron spectroscopy (XPS), X-ray diffraction (XRD), temperature-programmed desorption (TPD), and several other characterization techniques. The results of TPD of acetylene from the catalyst indicated that Au³⁺ has a negative influence on acetylene activation, but the surface functional groups play an important role. This could provide a new perspective on the reaction mechanism. Hutchings et al. have

* Corresponding author at: Key Laboratory of Advanced Energy Materials Chemistry (Ministry of Education), College of Chemistry, Nankai University, Tianjin 300071, China. Fax: +86 22 23508662.

E-mail address: weili@nankai.edu.cn (W. Li).

proposed that the efficiency of the catalyst is probably related to the location of Au³⁺ at the Au/C interface, and this is an important aspect so far neglected for the catalysts [11]. Thus, we demonstrated that the surface functional groups are a constituent part of the active site and provide a preliminary discussion on the role of each part.

2. Experimental

2.1. Catalyst preparation

A commercial activated carbon (extruded coconut carbon of diameter 1.5 mm and length 3–5 mm) was used as the starting material. The activated carbon was modified by thermal and chemical treatments in order to obtain supports with different surface chemical properties. Then all catalysts were prepared using an incipient wetness impregnation method.

2.1.1. Preparation of modified activated carbon

Pretreatment of activated carbon: Initially, activated carbon was crushed and the crushed particles between 20 and 60 mesh were sieved out for use. The selected materials were washed with distilled water at 60 °C for 3 h to remove the carbon dust attached to the activated carbon particles. Then the mixture was filtered, and then dried at 130 °C for 12 h (sample AC_{original}).

Thermal treatments of activated carbon: Supported AC_{original} was treated in an argon flow for 3 h at different temperatures (300, 600, and 900 °C) and then cooled to ambient temperature in situ. The obtained samples are referred to as AC₃₀₀, AC₆₀₀, and AC₉₀₀, respectively. Thermal treatments modified the activated carbon surface functional groups because no ions are introduced to the sample using this technique [17].

Acid treatment of activated carbon: Supported AC_{original} was soaked in HCl (2 M, 10 mL per 1 g activated carbon) or HF (2 M, 10 mL per 1 g activated carbon) at ambient temperature for 48 h, and then the obtained materials were filtered and washed with distilled water (2 L per 1 g activated carbon) until the water was near neutral pH. The obtained materials were dried at 130 °C for 10 h and are referred to as AC_{HCl} and AC_{HF}.

Oxidation and reduction of activated carbon: Supported AC_{original} was soaked in H₂O₂ (10 wt.%, 10 mL per 1 g activated carbon) at ambient temperature for 3 h, and then the obtained materials were filtered and washed with distilled water (2 L per 1 g activated carbon). The obtained materials were dried at 130 °C for 10 h and are referred to as AC_{H₂O₂}. Supported AC_{original} was treated in a H₂ or C₂H₂ flow for 3 h at 180 °C and then cooled to ambient temperature in an argon flow in situ. The obtained samples are referred to as AC_{H₂} and AC_{C₂H₂}, respectively.

2.1.2. Preparation of catalysts

Dilute aqua regia was used as the solvent for the catalyst preparation to reduce the effect of the concentrated aqua regia in oxidizing the surface functional groups on activated carbon. The gold precursor, HAuCl₄·4H₂O, was dissolved in dilute aqua regia (1:9 aqua regia:H₂O by volume, 16.4 mL), and then the solution was added dropwise with stirring to the pretreated support in order to obtain the catalyst with a final AuCl₃ loading of 1 wt.%. Stirring was continued at ambient temperature for half an hour and then the product was dried for 24 h at 130 °C [11,18]. The obtained catalysts are referred to as Cat_{original}, Cat₃₀₀, Cat₆₀₀, Cat₉₀₀, Cat_{HCl}, Cat_{HF}, Cat_{H₂O₂}, Cat_{H₂}, and Cat_{C₂H₂} according to the supports used in the preparation process.

2.2. Catalytic activity test

Catalysts used for acetylene hydrochlorination were tested in a fixed-bed microreactor. Ceramic rings (diameter 4 mm and length 4 mm) were used to extend the bed length above the catalysts (3.2 g, 10 mL), which could mix and preheat the reactant at the same time. Prior to the reaction, the catalysts were pretreated in situ with HCl (30 mL min⁻¹) at 180 °C for 1 h [9]. After that, HCl (66 mL min⁻¹) and C₂H₂ (60 mL min⁻¹) were fed to the heated reactor (180 °C) via calibrated mass flow controllers, with a C₂H₂ gas hourly space velocity (GHSV) of 360 h⁻¹. A blank experiment was carried out using an empty reactor filled with ceramic rings under the same conditions, and the ceramic rings did not show any catalytic activity. The gas phase products were analyzed on line using a gas chromatograph (GC) equipped with a thermal conductivity detector.

2.3. Characterization of catalysts

TPD analysis was carried out using a Micromeritics Chemisorb 2750 gas adsorption instrument equipped with a thermal conductivity detector. The sample (ca. 200 mg) was pretreated under N₂ at 130 °C for 2 h. After cooling in N₂, the sample adsorbed a probe gas for 1 h. Subsequently, the sample was purged for 30 min under N₂. Then the sample was treated under He for 1 h in order to replace N₂ in the instrumentation system. After that, the sample was heated to 900 °C at a rate of 10 °C min⁻¹ under He at a gas flow rate of 25 mL min⁻¹.

The Brunauer–Emmett–Teller (BET) specific surface area data were obtained using nitrogen adsorption/desorption measurements at 77 K with a BELSORP-Mini instrument. Powder XRD was performed on a Bruker D8 focus diffractometer with CuK α radiation at 40 kV and 40 mA. XPS was carried out using a PHI 1600 ESCA spectrometer equipped with an AlK α X-ray source (250 W) with an analyzer pass energy of 188 eV for survey scans and 30 eV for detailed elemental scans. The Fourier transform infrared radiation (FTIR) spectra were obtained using a Bio-Rad FTS 6000 spectrometer with 16 scans and a resolution of 8 cm⁻¹. The samples were prepared in KBr pellets. Atomic absorption spectroscopy (AAS) was performed using a TAS-990 instrument with an air–acetylene flame.

3. Results and discussion

3.1. Correlation between catalytic activity and C₂H₂ temperature-programmed desorption

The activity of the set of AuCl₃/C catalysts (Cat_{original}, Cat₃₀₀, Cat₆₀₀, and Cat₉₀₀) is reported in Fig. 1. The C₂H₂ GHSV and the feed volume ratio between HCl and C₂H₂ were chosen to test catalysts under mild conditions. It should be mentioned that for all of the activity tests carried out in the current study, the selectivity to VCM was virtually 100%, with only trace amounts of 1,2-dichloroethane and chlorinated oligomers [9].

It can be seen that all four AuCl₃/C catalysts exhibited unstable acetylene conversion (ca. 92%) in the first hour, and the activity eventually increased to about 97.5% in the second hour. However, the catalysts showed a decrease in C₂H₂ conversion (C₂H₂ conversion by Cat_{original}, Cat₃₀₀, Cat₆₀₀, and Cat₉₀₀ decreased ca. 5.67%, 5.79%, 1.70%, and 4.04%, respectively) after being followed for 7 h on stream, and Cat₆₀₀ exhibited the best stability (stability: Cat₆₀₀ > Cat₉₀₀ > Cat₃₀₀ \approx Cat_{original}). The deactivation of the AuCl₃/C catalysts tested at the reaction temperature (180 °C) was mostly due to reduction of the active gold species Au³⁺ to Au⁰, which is caused by the negative effects of C₂H₂ [8,10,19,20].

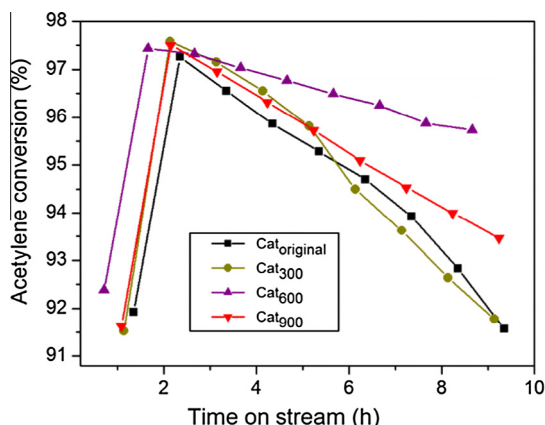


Fig. 1. Acetylene conversion by AuCl_3/C catalysts. Reaction conditions: temperature = 180°C , C_2H_2 GHSV = 360 h^{-1} , feed volume ratio between HCl and C_2H_2 = 1.1.

In order to gain insight into the interaction between the catalyst and reactant, C_2H_2 TPD of the catalysts was conducted (Fig. 2). It is worth noting that desorption peaks before 200°C have different areas in the order $\text{Cat}_{600} < \text{Cat}_{900} < \text{Cat}_{300} \approx \text{Cat}_{\text{original}}$, which is the opposite of the stability order.

To further identify the C_2H_2 desorption peak and investigate the effects between C_2H_2 and the surface functional groups, C_2H_2 TPD and a blank TPD of $\text{AC}_{\text{original}}$ were carried out (Fig. 3). In the blank TPD of $\text{AC}_{\text{original}}$, surface functional groups on activated carbon decompose upon heating by releasing CO and CO_2 at different temperatures. In general, a CO_2 peak results from carboxylic acids at low temperatures, or lactones at higher temperatures; carboxylic anhydrides produce both CO and CO_2 peaks; phenols, ethers, and carbonyls produce a CO peak [17]. Comparing these two TPD curves of $\text{AC}_{\text{original}}$ in Fig. 3, there are two obvious points that should be noted: (1) C_2H_2 desorption take place before the CO_2 or CO peaks increase and (2) in the curve of $\text{AC}_{\text{original}}-\text{C}_2\text{H}_2$, the amount of CO_2 and CO produced by decomposition of surface functional groups shows a significant decrease between 200 and 800°C , and the decomposition peak shifts toward high temperature. These results indicate that there are two interaction mechanisms between C_2H_2 and activated carbon: (1) the C_2H_2 desorbed before 200°C was adsorbed by activated carbon with weak interaction and (2) the decrease of CO_2 and CO may be because of the reaction between C_2H_2 and surface functional groups, which could inhibit the decomposition of those functional groups. The reaction

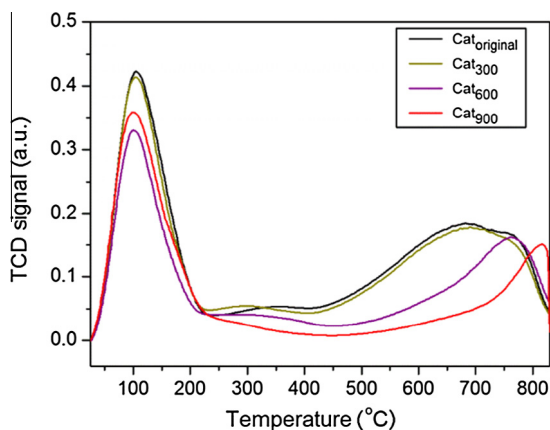


Fig. 2. C_2H_2 TPD on different AuCl_3/C catalysts.

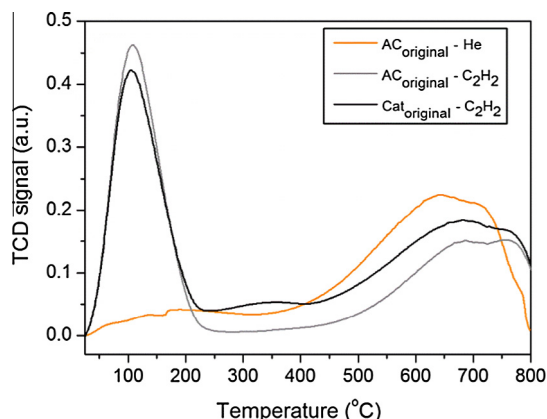


Fig. 3. C_2H_2 TPD and He TPD of the $\text{C}_{\text{original}}$.

between C_2H_2 and the surface functional groups changed C_2H_2 into other compounds, and this would not help the activation of C_2H_2 .

Considering that active carbons have strong physisorption, the amount of adsorbed C_2H_2 may be affected by the texture of the support. The BET surface area data are shown in Table 1. The surface area exhibited a decline with the increase in the pretreatment temperature, and this was caused by the decomposition of the surface functional groups under high temperatures [16]. But the amount of C_2H_2 adsorbed has no relationship to the surface area. For example, Cat_{300} and Cat_{600} are similar in surface area, pore volume, and pore diameter, but have obvious differences in C_2H_2 desorption peak area. Thus, we can conclude that the change of texture of activated carbon makes little contribution to the adsorption of C_2H_2 mentioned above.

In general, the desorption temperatures in the C_2H_2 TPD profiles reflect the binding strength of the adsorbed species on the catalyst surface, and the peak area correlates with the amount of adsorbed species. The C_2H_2 desorption peak is generally attributable to the ability of the catalyst to activate C_2H_2 directly [12,13,21,22]. Thus, we can conclude that the peaks below 200°C represent the adsorption and activation of C_2H_2 . This can explain the reverse order between catalyst stability and C_2H_2 adsorption capacity, because C_2H_2 leads to deactivation [9].

Otherwise, according to the C_2H_2 TPD of $\text{AC}_{\text{original}}$ and $\text{Cat}_{\text{original}}$, it seems that the addition of gold suppresses the two kinds of adsorption of acetylene. At the same time, we could find differences between the C_2H_2 TPD of the set of catalysts shown in Fig. 2. It is obvious that the peak area between 200 and 800°C decreased significantly with the increase in pretreatment temperature. This is mainly because the surface functional groups had decomposed in the pretreatment program, and the higher the pretreatment temperatures, the more decomposition of the functional groups.

For the peak below 200°C in Fig. 2, the desorption temperature and the peak area obtained from the set of catalysts are displayed in Table 2. A counterintuitive observation should be highlighted that the adsorption capacity of the active sites for activating C_2H_2 has a negative correlation with the catalyst stability. In other

Table 1
Surface area data for different AuCl_3/C catalysts.

Sample	Surface area ($\text{m}^2\text{ g}^{-1}$)	Total pore volume ($\text{cm}^3\text{ g}^{-1}$)	Average pore diameter (nm)
$\text{Cat}_{\text{original}}$	1006	0.79	3.13
Cat_{300}	1141	0.85	2.96
Cat_{600}	1098	0.81	2.95
Cat_{900}	997	0.73	2.93

Table 2
Desorption temperature and the peak area of the TCD signal of the set of catalysts.

Sample	Quality (g)	Desorption temperature (°C)	Peak area (TCD signal)
Cat _{original}	0.2003	105.3	33.32
Cat ₃₀₀	0.2000	104.6	32.14
Cat ₆₀₀	0.2003	100.9	22.65
Cat ₉₀₀	0.2000	100.0	28.10

words, we can assume that the activated carbon has outstanding ability to activate C₂H₂ and the addition of gold suppresses the adsorption and activation of acetylene.

In summary, activated carbon has the ability to activate C₂H₂ and work as a constituent part of the active site.

3.1.1. Existence of gold in the AuCl₃/C catalysts

Because the existence of Au³⁺ will determine the activity of the supported gold catalyst [11,23], the Au³⁺ may affect the adsorption of reactants for acetylene hydrochlorination. To test the existence of gold in the catalysts, XPS was systematically carried out for the catalysts (Fig. 4) (wide-scan spectra are shown in Fig. S1 in the Supplementary Material). It is evident that Cat₆₀₀ presented the highest signal intensity of Au, Cat₉₀₀ exhibited a lower signal intensity, and Cat_{original} and Cat₃₀₀ had the lowest intensity, which may represent a noisy signal. For these four catalysts, the loading of AuCl₃ is 1 wt.%, which means that the surface atomic percentage of Au may be less than 1% (the detection limit of XPS). This may be the main reason for the weak signals. However, Cat₆₀₀ presented the strongest signal, which means there are more gold atoms anchored on the surface of catalyst. The amount of Au⁰ is greater than that of Au³⁺. This may be because the Au³⁺ was undergoing reduction during XPS analysis.

Because XPS is a surface technique, we determined the gold loading using AAS, which showed that all of the catalysts have a total AuCl₃ loading of approximately 1 wt.%. In addition, XRD, which is also a bulk technique, was carried out in order to detect the gold content in the catalysts (Fig. 5).

According to the results of AAS (AuCl₃ content of Cat_{original}, Cat₃₀₀, Cat₆₀₀, and Cat₉₀₀: 0.97, 0.98, 0.96, and 0.98 wt.%), the content of gold in the AuCl₃/C catalysts is basically the same as the AuCl₃ loading of 1 wt.%. The catalysts were prepared using the incipient wetness impregnation method, which is known to be the most effective preparation method and guarantees that all of the gold precursor can be loaded onto the supports [3–5,10,11,18,24]. However, the XRD patterns show that Cat_{original} and Cat₃₀₀ have a stronger gold signal, which indicates larger gold particles. As for Cat₆₀₀, no discernible gold reflection was detected,

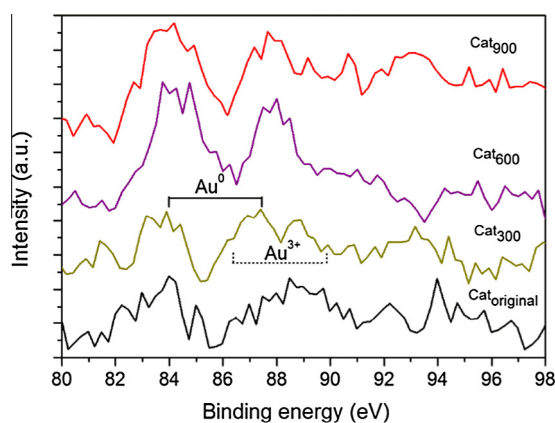


Fig. 4. XPS spectra of different AuCl₃/C catalysts.

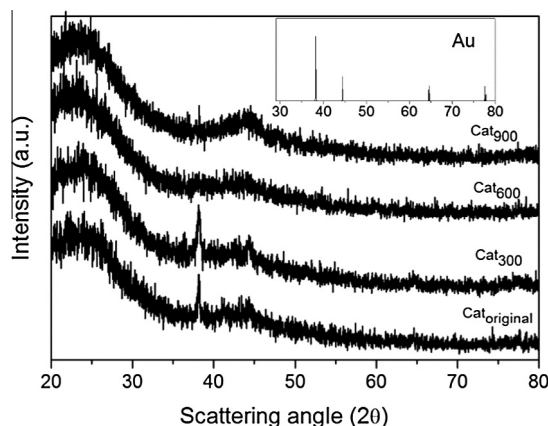


Fig. 5. XRD patterns of different catalysts.

indicating that the particles were smaller than 4 nm or the material had a large amount of Au⁰ and Au³⁺ distributed on the surface [11].

Considering all of the results of XPS, AAS, and XRD, it can be assumed the set of catalysts all have the same loading of Au. However, for Cat_{original} and Cat₃₀₀, sintering of gold was observed because the precursor, HAuCl₄, was reduced by the functional groups on the activated carbon and grew into nanoparticles in the absence of concentrated aqua regia as the solvent [11]. For Cat₆₀₀ and Cat₉₀₀, the functional groups were modified by a thermal method; consequently, less precursor was stirred into the Au nanoparticles and more Au⁰ and Au³⁺ were anchored on the surface of the active carbon, which may contribute to the activity and stability of the catalyst.

According to the report of Conte et al., an excess of Au³⁺ does not contribute to catalyst activity [11], which could explain the set of catalysts evaluated above having the same initial activity. However, combined with the results of C₂H₂ TPD and the deactivation rate of the catalysts, it is obvious that the greater the content of Au³⁺ or Au⁰ anchored on the surface, the less C₂H₂ is adsorbed and activated by the catalysts. This phenomenon decreased the reduction of Au³⁺ by C₂H₂ during the reaction, and thus improved the stability of the catalysts.

3.1.2. Effect of surface functional groups in the AuCl₃/C catalysts

According to these results, the gold existing on the surface of the catalysts suppresses the adsorption of C₂H₂, which means that gold and C₂H₂ may located in the same sites on the surface of catalysts. In order to investigate the effect of surface chemistry on C₂H₂ TPD, the catalysts were also characterized using FTIR and XPS.

FTIR was employed to explore the change in functional groups of different catalysts (Fig. 6). The relative intensities of all of the broad peaks decreased with increased treatment temperatures. At 900 °C there is a significant decrease in all of the relevant peaks, which indicates the decomposition of all the functional groups. This phenomenon could also be demonstrated by the C₂H₂ TPD results (Fig. 2), where the surface area between 200 and 850 °C decreased with increased treatment temperature.

Because the Cat₉₀₀ reveals inconspicuous peaks in its FTIR spectrum, XPS analysis was obtained only for the other three catalysts. Atomic ratios of the three catalysts are shown in Table 3. The atomic ratios of O1s exhibited a decline with increase in the pre-treatment temperature, and this indicated the decomposition of the surface functional groups at high temperatures. Cat₆₀₀ had the highest atomic ratios of Au4f, which is consistent with the discussion in Section 3.1.1.

XPS spectra of the C1s region of the catalysts are shown in Fig. 7. Carbon atoms differ in their binding energy depending on whether

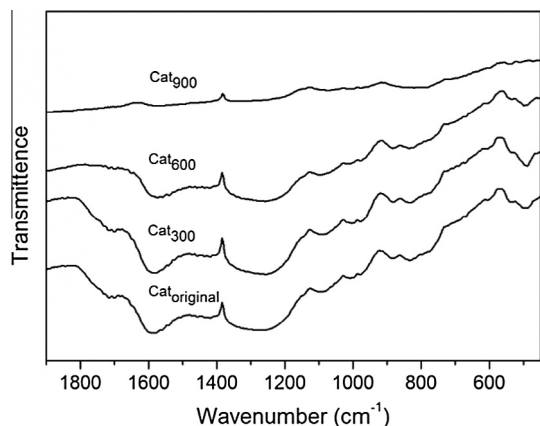


Fig. 6. FTIR spectra of different catalysts.

Table 3

Atomic ratios of C1s, O1s, and Au4f of different catalysts.

Sample	C1s (%)	O1s (%)	Au4f (%)
Cat _{original}	82.57	17.41	0.02
Cat ₃₀₀	84.16	15.83	0.01
Cat ₆₀₀	90.30	9.66	0.04

they are linked to one O atom by a single bond or a double bond or to two or three oxygen atoms [25]. Thus, deconvolution of the C1s spectra gives five individual component peaks [26,27]: peak I (284.6 eV, which represents graphitic carbon), peak II (286.1–286.3 eV, representing carbon present in phenolic or alcohol groups), peak III (287.3–287.6 eV, representing carbonyl or quinone groups), peak IV (288.4–288.9 eV, representing carboxyl or ester groups), and peak V (290.4–290.8, carbon present in carbonate groups and/or adsorbed CO or CO₂).

Comparing the spectrum of Cat₆₀₀ with the spectra of Cat_{original} and Cat₃₀₀, there was a significant decrease in the relative content of phenolic or alcohol groups (peak II) and carbonyl or quinone groups (peak III), and there was an increase in peak I. This may be explained by assuming that as the treatment temperature increased, the surface functional groups decomposed into CO or CO₂. But the amount of carboxyl (peak V) decreased only slightly from 4.19% to 3.75%. This result may be because of using dilute aqua regia in the process of preparation of catalysts, by which part of other function groups (peak II or peak III) oxidized into carboxyl (peak V).

Fig. 8 shows the O1s spectra fitted to three component peaks [26,28]: peak I (531.1–531.7 eV, representing C=O groups: ketone, lactone, and/or carbonyl); peak II (533.1–533.4 eV, representing C–OH and/or C–O–C groups); peak III (535.5–535.9 eV, representing chemisorbed oxygen and perhaps some adsorbed water). Regardless of peak III, the content of peak I and peak II in each catalyst is listed: Cat_{original} (peak I, 30.46%, peak II, 69.54%), Cat₃₀₀ (peak I, 32.82%, peak II, 67.18%), Cat₆₀₀ (peak I, 46.72%, peak II, 53.28%). Although XPS is a semiquantitative technique, by combining spectra of C1s, we can find out that Cat₆₀₀ possesses the highest relative content of ketone, lactone, and/or carbonyl (peak I in spectra of O1s) and the lowest relative content of phenolic and/or alcohol groups (peak II in spectra of C1s). At the same time, for Cat₆₀₀, less precursor, HAuCl₄, was stirred into the Au nanoparticles and more gold atoms were anchored on the surface of the active carbon (part of Au⁰ may be due to the Au³⁺ undergoing reduction during XPS analysis). These results are consistent with the theory first reported by Davies et al. that ketone, lactone, and/or carbonyl tend to anchor gold in a surface with a good dispersion state that is

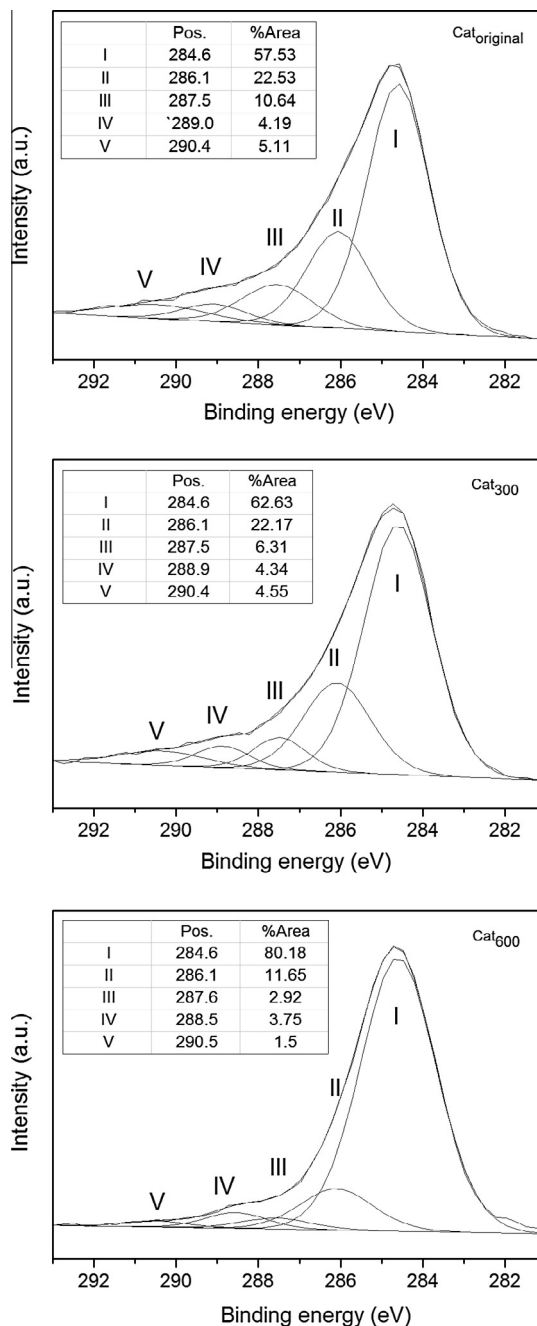


Fig. 7. XPS C1s spectra of the different catalysts.

useful for the reaction, while phenolic and/or alcohol groups easily reduce Au³⁺ into Au⁰ in the form of nanoparticles, which is useless for the reaction [28]. It also demonstrated that the efficiency of the catalyst is likely to be related to the location of Au³⁺ at the gold/carbon interface of the catalyst [11].

It has been reported that the interaction between a hydrogen atom of C₂H₂ and an oxygen atom of microporous materials is based not only on electrostatic attraction but also on the electron delocalization effect [29]. Combined with the results of C₂H₂ TPD and the stability of catalysts, it may be assumed that groups such as ketone, lactone, or carbonyl play the main role in the adsorption of C₂H₂. It can be further demonstrated that the surface functional groups in the AuCl₃/C catalyst are a constituent part of the active site, having a role in adsorbing and activating one of the reactants. However, because the functional groups have effects on gold

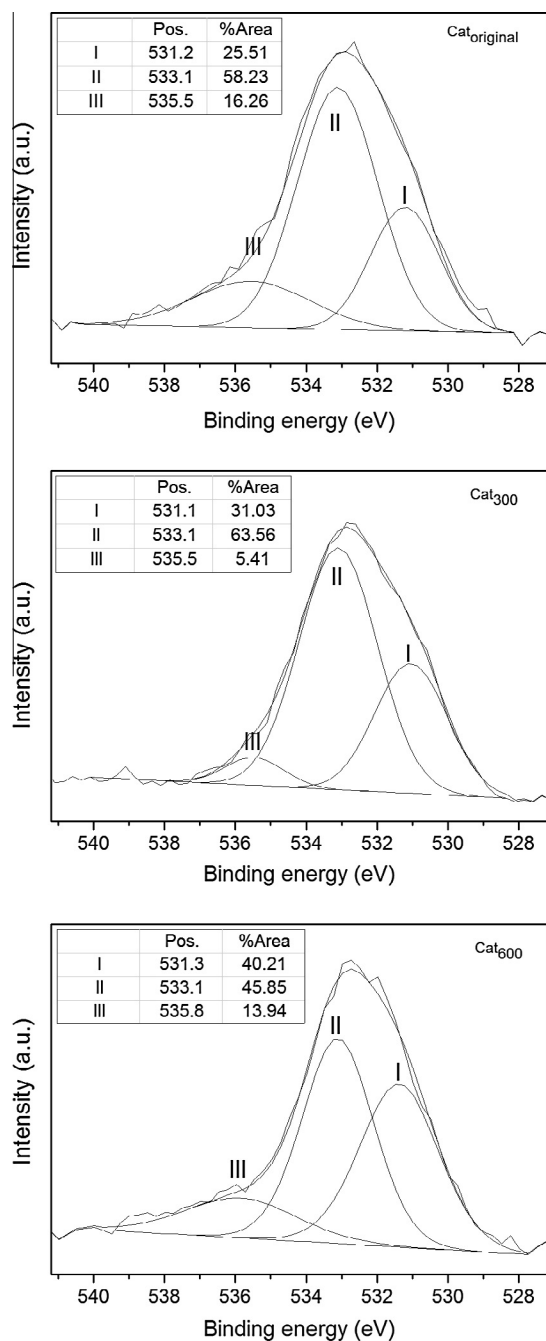


Fig. 8. XPS O1s spectra of the different catalysts.

desorption [28], and because of the limitations of the characterization techniques, a detailed mechanism for activating C_2H_2 is still unclear.

3.2. Other evidence for the assumption of the active site

3.2.1. Effect of Cl^-

Activated carbon has excellent ability to activate C_2H_2 , and it could be further predicted that improving the ability of HCl to adsorb and activate will improve the performance of the $AuCl_3/C$ catalyst. It has been reported that preactivating the catalyst with HCl before the reaction and improving the feed proportion of HCl can improve the performance of the $AuCl_3/C$ catalyst

[9]. Considering this, pretreatment with Cl^- may have a positive effect on the catalyst performance.

Catalysts prepared using activated carbon pretreated with HCl and HF were evaluated (Fig. 9), and the C_2H_2 TPD of the catalysts was characterized. Compared with $Cat_{untreated}$ and Cat_{HF} , the initial activity of Cat_{HCl} increased dramatically and the stability was basically the same. From the results of C_2H_2 TPD (Fig. 10), Cat_{HCl} possessed the maximum peak area among those spectra.

Treatment of activated carbon with HCl and HF resulted in the removal of inorganic constituents that may poison the catalyst. It is obvious from the texture of Cat_{HCl} and Cat_{HF} (Table 4) that there is a significant reduction in ash content and an enhancement of BET surface area and total pore volume of the activated carbon. It is reported that HCl generally increases the surface oxygen content, whereas HF decreases the surface oxygen content [30]. This may explain the maximum C_2H_2 adsorption peak area of Cat_{HCl} . However, the observation that Cat_{HCl} possesses the highest initial activity may be ascribed to the effect of the Cl^- , and this was consistent with the assumption.

3.2.2. Controllable modulation of the induction period of the catalyst

In acetylene hydrochlorination, there will be an induction period before the catalyst reaches the highest activity [7,18,23,31]. The induction period may be related to adsorption and diffusion of the reactants, the formation of the active sites, etc. For those $AuCl_3/C$ catalysts, we conjectured that the induction period

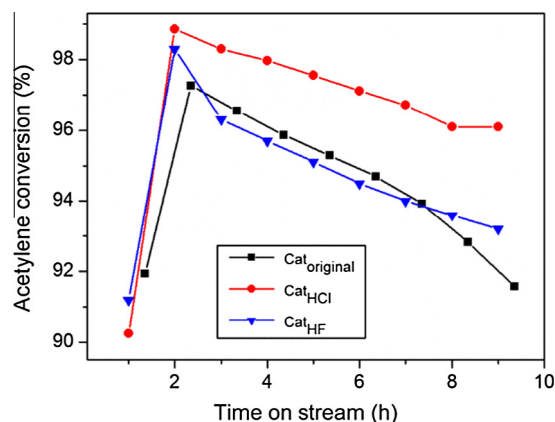


Fig. 9. Acetylene conversion by $AuCl_3/C$ catalysts. Reaction conditions: temperature = $180^\circ C$, C_2H_2 GHSV = $360\ h^{-1}$, feed volume ratio between HCl and C_2H_2 = 1.1.

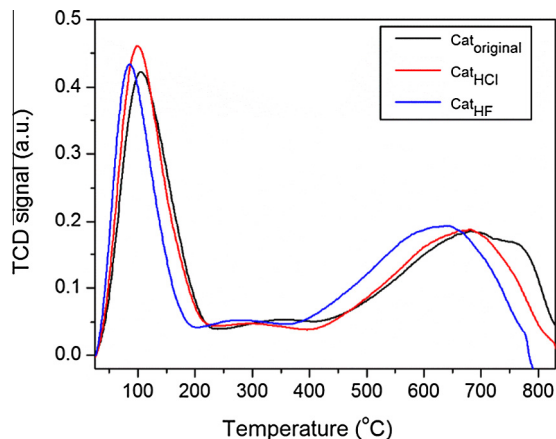


Fig. 10. C_2H_2 TPD on different $AuCl_3/C$ catalysts.

Table 4
Textural properties of different AuCl₃/C catalysts.

Sample	Surface area (m ² g ⁻¹)	Total pore volume (cm ³ g ⁻¹)	Average pore diameter (nm)	Ash (%)
Cat _{original}	1006	0.79	3.13	5.24
Cat _{HCl}	1030	0.82	3.03	3.71
Cat _{HF}	1037	0.84	3.08	2.56

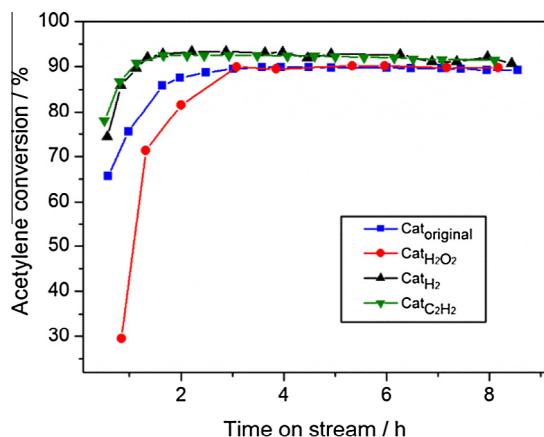


Fig. 11. Induction period of AuCl₃/C catalysts for acetylene hydrochlorination. Reaction conditions: temperature = 180 °C, C₂H₂ GHSV = 480 h⁻¹, feed volume ratio between HCl and C₂H₂ = 1.

represents a process of formation of active sites. We assumed that the formation of active sites is due to the modification of the functional groups by reducibility of C₂H₂. Thus, we pretreated activated carbon with H₂, C₂H₂, and H₂O₂ in order to modify surface functional groups and modulate the induction period of the catalyst.

To reduce the influence of the catalyst filling amount on the induction period, the set of catalysts (Cat_{original}, Cat_{H₂O₂}, Cat_{H₂}, and Cat_{C₂H₂}) were tested in a smaller fixed-bed microreactor (the reactors are shown in Fig. S2 in the Supplementary Material). Silica sand was used to extend the bed length above the catalysts (0.4 g, 1.25 mL), which could mix and preheat the reactant at the same time. Prior to the reaction, the catalysts were pretreated in situ with HCl (5 mL min⁻¹) at 180 °C for 1 h. After that, HCl (10 mL min⁻¹) and C₂H₂ (10 mL min⁻¹) were fed into the heated reactor (180 °C) via calibrated mass flow controllers, with a C₂H₂ GHSV of 480 h⁻¹. A blank experiment was carried out using an empty reactor filled with silica sand under the same conditions, and the ceramic rings did not show any catalytic activity. The gas phase products were analyzed on line using a GC equipped with a thermal conductivity detector.

The results are shown in Fig. 11. It was obvious that the reduction treatment shortened the induction period and the oxidation treatment increased the induction period. This result suggested that the reduction treatment could form the functional groups, which were part of the active sites before the reaction.

Because of the complexity and particularity of activated carbon materials, and the limitations of the characterization techniques, the study on the effect of Cl⁻ and the induction period of the catalysts needs more effort. But it could provide circumstantial evidence for the assumption that the surface functional groups were a constituent part of the active site adsorbing and activating C₂H₂.

4. Conclusions

Thermal treatments would change the surface functional groups on activated carbon. Ketone, lactone, and/or carbonyl tend

to anchor gold on the surface with a good dispersion state. The phenolic and/or alcohol groups can easily reduce Au³⁺ to Au⁰ in the form of nanoparticles. The catalyst with the best dispersibility of gold exhibits the best stability, but the adsorption capacity of the active sites for activating C₂H₂ has a negative correlation with the catalyst stability and gold dispersibility. This phenomenon indicates that the gold dispersed on the surface of activated carbon is not the active site for activating C₂H₂.

It seems that the surface functional groups may be a constituent part of the active sites adsorbing and activating C₂H₂. The support of Au on the activated carbon has a negative effect on the adsorption of C₂H₂. This may indicate that Au³⁺ and the surface functional groups work in synergy as the active sites. Thus, we can change our understanding of the reaction mechanism of acetylene hydrochlorination and change the design of the catalyst.

Acknowledgments

This work was financially supported by the NSFC – China (21376123, U1403293), MOE – China (IRT-13R30 and 113016A), and the Research Fund for 111 Project (B12015).

Appendix A. Supplementary material

Supplementary data associated with this article can be found, in the online version, at <http://dx.doi.org/10.1016/j.jcat.2015.07.008>.

References

- [1] X. Li, M. Zhu, B. Dai, Appl. Catal. B 142–143 (2013) 234.
- [2] K. Zhou, J.C. Jia, X.G. Li, X.D. Pang, C.H. Li, J. Zhou, G.H. Luo, F. Wei, Fuel Process. Technol. 108 (2013) 12.
- [3] B. Nkosi, N.J. Coville, G.J. Hutchings, Chem. Commun. (1988) 71.
- [4] B. Nkosi, M.D. Adams, N.J. Coville, G.J. Hutchings, J. Catal. 128 (1991) 378.
- [5] B. Nkosi, N.J. Coville, G.J. Hutchings, Appl. Catal. 43 (1988) 33.
- [6] G. Hutchings, J. Catal. 96 (1985) 292.
- [7] M. Conte, C.J. Davies, D.J. Morgan, T.E. Davies, A.F. Carley, P. Johnston, G.J. Hutchings, Catal. Sci. Technol. 3 (2013) 128.
- [8] M. Conte, A.F. Carley, G.J. Hutchings, Catal. Lett. 124 (2008) 165.
- [9] M. Conte, A.F. Carley, C. Heirene, D.J. Willock, P. Johnston, A.A. Herzing, C.J. Kiely, G.J. Hutchings, J. Catal. 250 (2007) 231.
- [10] B. Nkosi, N.J. Coville, G.J. Hutchings, M.D. Adams, J. Friedl, F.E. Wagner, J. Catal. 128 (1991) 366.
- [11] M. Conte, C.J. Davies, D.J. Morgan, T.E. Davies, D.J. Elias, A.F. Carley, P. Johnston, G.J. Hutchings, J. Catal. 297 (2013) 128.
- [12] X. Li, Y. Wang, L. Kang, M. Zhu, B. Dai, J. Catal. 311 (2014) 288.
- [13] X. Li, X. Pan, L. Yu, P. Ren, X. Wu, L. Sun, F. Jiao, X. Bao, Nat. Commun. 5 (2014) 3688.
- [14] X. Li, X. Pan, X. Bao, J. Energy Chem. 23 (2014) 131.
- [15] K. Zhou, B. Li, Q. Zhang, J.Q. Huang, G.L. Tian, J.C. Jia, M.Q. Zhao, G.H. Luo, D.S. Su, F. Wei, ChemSusChem 7 (2014) 723.
- [16] E.G. Rodrigues, M.F.R. Pereira, X.W. Chen, J.J. Delgado, J.J.M. Orfao, J. Catal. 281 (2011) 119.
- [17] J.L. Figueiredo, M.F.R. Pereira, M.M.A. Freitas, J.J.M. Orfao, Carbon 37 (1999) 1379.
- [18] W. Wittanadecha, N. Laosiripojana, A. Ketcong, N. Ningnuek, P. Praserttham, J.R. Monnier, S. Assabumrungrat, Appl. Catal. A 475 (2014) 292.
- [19] J.M. Ma, S.J. Wang, B.X. Shen, React. Kinet. Mech. Catal. 110 (2013) 177.
- [20] S.J. Wang, B.X. Shen, Q.L. Song, Catal. Lett. 134 (2010) 102.
- [21] J. Zhao, J. Xu, J. Xu, J. Ni, T. Zhang, X. Xu, X. Li, ChemPlusChem 80 (2015) 196.
- [22] C. Zhang, L. Kang, M. Zhu, B. Dai, RSC Adv. 5 (2015) 7461.
- [23] M. Conte, C.J. Davies, D.J. Morgan, A.F. Carley, P. Johnston, G.J. Hutchings, Catal. Lett. 144 (2014) 1.
- [24] M. Conte, A.F. Carley, G. Attard, A.A. Herzing, C.J. Kiely, G.J. Hutchings, J. Catal. 257 (2008) 190.
- [25] H.P. Boehm, Carbon 40 (2002) 145.
- [26] Z.R. Yue, W. Jiang, L. Wang, S.D. Gardner, C.U. Pittman Jr., Carbon 37 (1999) 1785.
- [27] S.D. Gardner, C.S.K. Singamsetty, G.L. Booth, G.-R. He, C.U. Pittman Jr., Carbon 33 (1995) 587.
- [28] R. Burgess, C. Buono, P.R. Davies, R.J. Davies, T. Legge, A. Lai, R. Lewis, D.J. Morgan, N. Robinson, D.J. Willock, J. Catal. 323 (2015) 10.
- [29] R. Matsuda, R. Kitaura, S. Kitagawa, Y. Kubota, R.V. Belosludov, T.C. Kobayashi, H. Sakamoto, T. Chiba, M. Takata, Y. Kawazoe, Y. Mita, Nature 436 (2005) 238.
- [30] S.B. Wang, G.Q. Lu, Carbon 36 (1998) 283.
- [31] C. Huang, M. Zhu, L. Kang, X. Li, B. Dai, Chem. Eng. J. 242 (2014) 69.